

Qualitative model of high- T_c superconductivity

Nikolai A. Zarkevich*

Ames Laboratory, U.S. Department of Energy, Ames IA 50011, USA

(Dated: October 12, 2018)

We suggest a qualitative model of a high- T_c superconductor, based on considerations of thermodynamics of phase transitions. As an example, we consider the Mott transition and classify 5 solid phases around it. In our model, a combined electronic and structural instability causes segregation into either neutral or charged phases. A charged precipitate with a quantized electric charge is a collective excitation of electrons, stabilized by a collective athermal displacement of ions; this local variation of the charge density, accompanied by a local lattice deformation, can behave as a quasi-particle. A condensate of charged bosonic quasiparticles is responsible for the superconductivity.

PACS numbers: 74.20.-z, 74.25.Dw, 64.75.Jk, 74.81.-g, 74.20.Mn

Keywords: Mott, superconductivity, phase transition, segregation

INTRODUCTION

Materials on the edge of their stability can have enormous lattice response to a perturbing field. A responsive lattice is necessary for such phenomena as, for example, a giant caloric effect or a high- T_c superconductivity.

A first-order phase transformation happens between two phases of unequal density. Phases can coexist at equal pressure P , temperature T , and chemical potential μ . Volume V [\AA^3 per formula unit (f.u.)], interatomic distances d_a [\AA], density ρ [g/cm^3], and local electronic [\AA^{-3}] and charge [$e^-/\text{\AA}^3$] densities are discontinuous at a 1st-order phase transition. Intermediate structures between the two phases are unstable; their segregation into the stable phases lowers the total Gibbs free energy G .

In our model, we consider a high- T_c superconductor as a phase-segregated material. In this neutral material both phases are charged, but the volume of one phase is much smaller than that of the other. The charged phase with small volume has a high charge density, and the Coulomb repulsion fractures it into tiny precipitates, which behave as quasiparticles, with a quantized electric charge. In conventional superconductors, such quasiparticles are known as the Cooper pairs, composed by a collective motion of electrons and a lattice deformation, which binds an even number of electrons (fermions) into one charged quasiparticle (boson).

Conventional superconductivity [1–3] happens due to electron-phonon coupling [4–8]. More generally, superconductivity (both conventional and unconventional) happens due to coupling between a collective electronic excitation and a lattice response to it, which is a collective athermal displacement of atoms and ions. Lattice deformations are responsible for coupling fermions (electrons) into bosons, and a Bose-Einstein condensate [9] of charged quasiparticles is responsible for the superconductivity. A larger lattice response can result in a larger critical temperature T_c . Hence, a guided search for high- T_c superconductors starts with a study of electronic and lattice instabilities.

A high- T_c superconductivity occurs around an instability. Electronic and structural instabilities result in phase transformations. One of them is the Mott transition [10].

The Mott transition is electronic by nature. It happens due to a change of electronic structure, accompanied by a change in interatomic interactions, which drive atoms to their new equilibrium positions, thus relaxing interatomic distances d_a , volume V , and density ρ . At the same external stress, temperature, and composition, two different electronic states have equilibrium at different lattice constants. Any intermediate crystal structures between those two terminal equilibria are not stable: they are destined to transform. What is the speed of electronic and structural transformations?

Electromagnetic interactions, including those between electrons, propagate with the speed of light $c_{light} \approx 3 \times 10^8$ m/s. Fermi velocity of conductive electrons in a metal is $v_F \sim 10^6$ m/s (e.g., 1570 km/s in copper). Lattice vibrations (phonons) propagate with the speed of sound $v_{sound} \sim 10^3$ m/s (e.g., 4760 m/s for longitudinal waves in an annealed copper [11] at room T).

In contrast, drift velocity $u_D = J/qn_q$ of carriers with charge q and concentration n_q in a conductor with current density $J = I/S$ is very modest. For example, in a copper wire ($n_q = 8.5 \times 10^{28} \text{ m}^{-3}$) with a cross section $S = 1 \text{ mm}^2$ at constant direct current $I = 1 \text{ A}$, drift velocity of electrons constitutes only 7×10^{-5} m/s.

In a superconductor, each charged bosonic quasiparticle is accompanied (and held together) by a local lattice deformation, which follows its drift. From the other hand, thermal atomic motion disturbs such a local lattice deformation, which acts as a “glue” for the quasiparticle. Without such a “glue”, those quasi-particles can no longer exist, and superconductivity is destroyed above the critical temperature T_c . A larger lattice response results in a higher T_c . In general, the lattice response is the largest near phase transitions. The quantum critical point (QCP) is an example of a phase boundary at 0K.

Below we propose a model of superconductivity in the vicinity of a phase boundary. This model can help in a

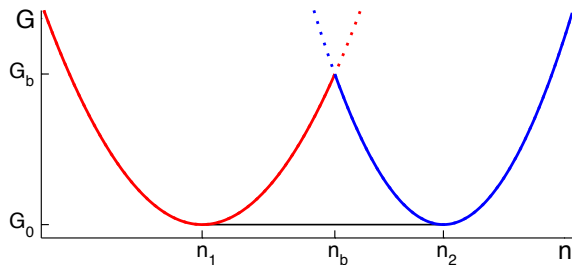


FIG. 1. Gibbs free energy G of two phases (1 and 2) versus average electronic density n . Its change Δn can be comprehended as a level of doping. The tangent (black line) is horizontal, if two segregated phases are at a thermal equilibrium.

guided search for novel high- T_c superconductors.

THEORETICAL MODEL

Let us consider a bulk solid with an instability, resulting in phase transformations. Such transformations can be driven by changing temperature T , pressure P , composition c (and hence chemical potential μ), average electronic density n , or the level of doping Δn .

Instability in electronic density

Let us expand the Gibbs free energy $G(T, P, c, n)$ at fixed $\{T, P, c\}$ in a Taylor series around its minimum in each phase $i = \{1, 2\}$:

$$G_i(n) = G_i^{(0)} + (\partial^2 G_i / \partial n^2)(n - n_i)^2 + O(n - n_i)^3. \quad (1)$$

The mixture of phases with the same n has

$$G(n, x_i) = \sum_i x_i G_i(n), \quad (2)$$

where x_i is the i -phase fraction, and

$$\sum_i x_i = 1. \quad (3)$$

At thermodynamic equilibrium, $G_2^{(0)} = G_1^{(0)} \equiv G_0$. Neglecting the higher-order terms $O(n - n_i)^3$, we get:

$$G(n, x_1) \approx G_0 + x_1(n - n_1)^2 G_1^{(2)} + (1 - x_1)(n - n_2)^2 G_2^{(2)} \quad (4)$$

If both phases are stable, then $G_i^{(2)} \equiv (\partial^2 G_i / \partial n^2)_{n_i} > 0$. We can generalize consideration to any continuous curves $G_i(n)$ with minima at $G_i(n_i) = G_i^{(0)}$; each curve is convex at the minimum n_i and monotonic on both sides (decreases at $n < n_i$ and increases at $n > n_i$), see Fig. 1.

Without a loss of generality, let us assume $n_1 < n_2$ (i.e., we label the phase with lower n by index 1). Then

for any intermediate electronic density $n_1 < n < n_2$, segregation into two phases with electronic densities n'_1 and n'_2 , where $n_1 < n'_1 < n_b$ and $n_b < n'_2 < n_2$, results in the lowering of G , and is favorable, see Fig. 1.

Instability is repulsive

Obviously, electronic and lattice structure at the instability is unstable, while it becomes more stable further from the instability. Increased “distance” from the instability in terms of the phase space coordinates results in lower G . Thus, instability is “repulsive” in the phase space. This is illustrated by Fig. 1, where $G_b(n_b)$ is the instability, and n is a phase space coordinate. The “repulsive” region is at $n_1 < n < n_2$.

Superconductivity due to charged segregation

Again, one way to move away from the instability in terms of electron charge density n or doping Δn is a charge density segregation, which leads to creation of charged precipitates.

Let us consider a charged phase with a fixed total volume V_Q and fixed total charge Q . If this phase is allowed to fracture to $N_q = Q/q$ small precipitates of charge q , then its total potential energy $U \sim q^{2/3} Q^{4/3} V_Q^{-1/3}$ will be minimal for the smallest q , which nevertheless cannot be smaller than a certain quantum limit. This leads to quantum charges q of the precipitates, which can behave as quasiparticles. If these quasiparticles are bosons, then they can form a Bose-Einstein condensate [9] at low T . A condensate of charged bosonic quasiparticles is responsible for superconductivity.

Charged quasiparticles repel each other. This repulsion distributes them uniformly (in the absence of external fields), and can order them into a “quasilattice” (a geometric lattice-like arrangement of quasiparticles).

Without doubt, a variation of an electronic structure and charge density causes a lattice deformation. From the other hand, a local lattice deformation causes a local variation of the electronic structure: this reminds “the chicken and the egg” problem. Charged precipitates are so small, that they must be coherent with the lattice, but this coherency does not prevent them from creating a local strain. Symmetry of d_a distribution around a quasiparticle in a superconductor differs from a thermal distribution of interatomic distances, especially at low T . This lattice deformation could be detected in experiment using diffraction of x-rays or neutrons.

Magnetism

The role of magnetism in the high- T_c superconductors is still debatable. Typically there are several competing magnetic orderings around the instability, and the border between those spin states is also an instability of the electronic structure. Our model is applicable to any electronic instability. To remain generic, we do not restrict our consideration to a particular kind of instability, which might [12, 13] or might not [14] be magnetic.

MOTT TRANSITION

An example of a phase transformation, which changes topology of the electronic structure (Fig. 2), is the Mott transition. Figs. 3 and 4 show 5 distinctive phases: metal ($E_{gap} < 0$), a small-gap semiconductor ($0 < E_{gap} < k_B T$), insulator ($E_{gap} > k_B T$), and two superconducting phases at $T < T_c(E_{gap}) \leq T_S$ on both sides of the instability at the phase transition at $E_{gap} \equiv 0$, which is of the first-order at $0 \leq T \leq T_M$. Again, Fig. 3 shows one instability and 5 different solid phases around it. Some of those phases can be uniform, while others (including both CS) are segregated states.

Neutral and Charged Segregation

Mott transition is accompanied by both electronic and lattice instability. Fig. 4 shows a shaded region, where crystal structures are unstable. Such unstable structures segregate into charge-neutral stable phases of higher and lower density (ρ , as well as V and d_a).

In addition, the blue line in Fig. 4 is the border of a region of electronic instability, where the electronic structure wants to segregate into charged regions of higher

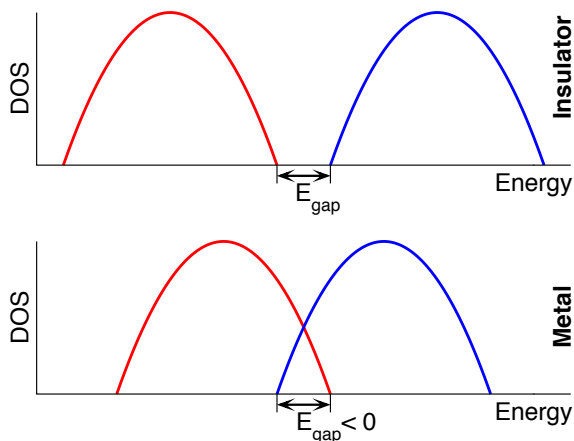


FIG. 2. Transformation between an insulator (with a band gap $E_{gap} > 0$) and a metal (with a band overlap, $E_{gap} < 0$).

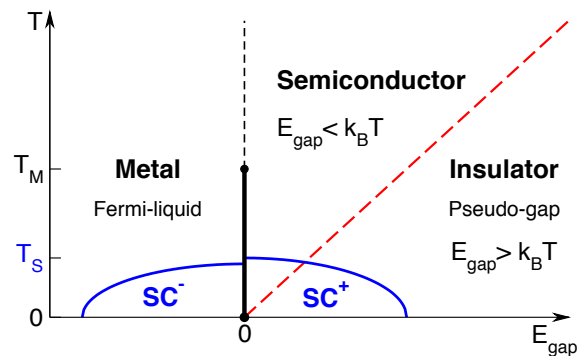


FIG. 3. Temperature T vs. the band gap E_{gap} near the Mott transition. Mott transition is 1st-order below the critical point at T_M . Superconducting state (SC) appears at low $T \leq T_S = \max(T_S^-, T_S^+)$. In a metal, $E_{gap} < 0$ is an overlap of bands, which changes monotonically with a finite electronic density at the Fermi level for small overlaps. Material with a band gap $E_{gap} > 0$ is either an insulator or a semiconductor, which conducts electricity if $E_{gap} < k_B T$.

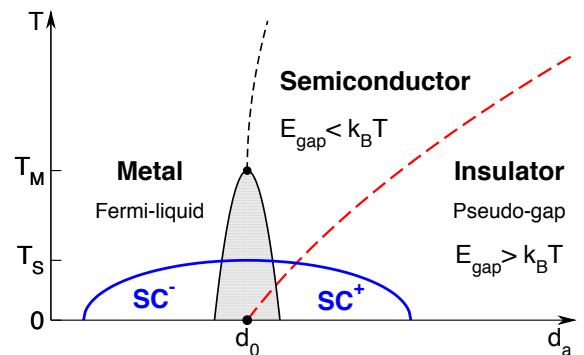


FIG. 4. Temperature T vs. characteristic interatomic distance d_a near the Mott transition. For two phases with different electronic structure at thermodynamic equilibrium, there is a gap in d_a , as well as lattice constants, density, and unit cell volume below T_M . The QCP at $(d_0, T=0)$ is in this gap. On the two sides of the gap, T_S^- and T_S^+ can differ.

and lower electronic density n , and above we provided a model explaining why this segregation is energetically favorable. Superconductivity is a result of this charged segregation. Conservation of electric charge (and consequently charge neutrality of the whole system) is an additional constraint, imposed on charged segregation.

Comparison to other diagrams

Figs. 3 and 4 are generic phase diagram for the Mott transition. A compatible T - P diagram for a compressible lattice is shown in Fig. 1 in [15], while the gap in strain and d_a is shown in their Fig. 4. Generic T - c diagrams in Fig. 1 in [16] and Fig. 2 in [17] show the small-gap semiconductor (at $0 < E_{gap} < k_B T$) as a “strange metal”.

Early attempts to draw a generic diagram may contain errors. In particular, Fig. 150 in [18] provides a schematic phase diagram of pseudogap structure in high- T_c cuprates, but it does not show a QCP at $T = 0$ K.

COMPARISON TO EXPERIMENT

In theory, phase diagrams showing T versus a phase-space variable x such as the band gap E_{gap} (Fig. 3), overlap of electronic orbitals, characteristic interatomic distance d_a (Fig 4), average electronic density n , or its change Δn , should be comparable regardless of the cause of variation of x . Examples of such causes are variations of composition c or applied pressure P [19]. Indeed, experiment [20] shows similarities between structural distortions under pressure and chemical doping in superconducting BaFe_2As_2 . Similar effects are found in SrFe_2As_2 doped by Co [21] and CaFe_2As_2 doped by Sr [22].

Examples of experimental T - c phase diagrams are Fig. 6 in [23] for the electron-doped $\text{Ba}(\text{Fe}_{1-x}\text{Co}_x)_2\text{As}_2$, Fig. 1 in [24] for $\text{Ba}_{1-x}\text{Rb}_x\text{Fe}_2\text{As}_2$, Fig. 4 in [25] for $\text{Ba}(\text{Fe}_{1-x}\text{Co}_x)_2\text{As}_2$, and Fig. 1d in [26] for $\text{CeFeAsO}_{1-x}\text{F}_x$. Examples of experimental T - P diagrams are Fig. 3 in [27] for SrFe_2As_2 , or Fig. 3 in [16] for $\text{Fe}_{1.01}\text{Se}$. Structural instability and superconductivity in $\text{SrNi}_2(\text{P}_{1-x}\text{Ge}_x)_2$ solid solutions was studied in [28]. Magnetic and structural transitions of SrFe_2As_2 at high P were investigated in [27]. Experiment finds that superconductivity happens around an instability, and theory claims that it happens due to an instability.

DISCUSSION

Two types of superconductivity

Our model of a charged segregation predicts that charges q of tiny precipitates (quasiparticles) should be quantized (e.g., $q = 2e$ for the Cooper pair), but it allows both signs of q . Hence, we anticipate existence of two distinctive types of superconductivity with positive and negative q . Here one can find similarity to two types semiconductors: p- and n-type. However, charge carriers in semiconductors can be fermions, while in a SC they are bosons. Two distinctive types of superconductivity are labeled SC^- and SC^+ in Figs. 3 and 4.

Collective excitations

We mentioned that electrons move much faster than their collective excitations. In particular, in a metal the Fermi velocity of electrons $v_F \sim 10^6$ m/s is huge compared to the drift velocity of charge carriers $u_D \ll 10^{-3}$ m/s. Thus, all quasiparticles in a superconductor

(including the Cooper pair) are collective electronic excitations, which should not be confused with propagation of a pair of particular electrons. Electrons in this collective excitation change, but the charge of the excitation and its total spin (responsible for bosonic behavior) remain constant.

Each quasiparticle is a collective electronic excitation (which locally changes the charge density), accompanied by a lattice deformation. Its motion with a small drift velocity u_D is accompanied by equally slow motion of that lattice deformation. Particular atoms or ions vibrate around their lattice positions; they do not follow the quasiparticle. However, a local change in density can be positive or negative; it is responsible for the mass of a quasiparticle.

There is a coupling between a collective electronic excitation and a collective atomic displacement. An electron-phonon coupling is one type of such coupling, but not the only one.

Lattice deformations and Phonons

Conventional superconductivity [1–3] happens due to electron-phonon coupling [4–8]. However, not every lattice deformation can be explained in terms of phonons. In particular, atomic positions in one phase are not always related to phonons in another phase in a phase-segregated material. Next, phonons are (quasi)harmonic vibrations of atoms, but not every collective atomic motion in a solid is harmonic. Hence, there are several reasons, why conventional theory of superconductivity might fail in several classes of “unconventional” superconductors.

From the other hand, our description of a superconductor as a phase segregated material with charged segregation is applicable to both conventional and high- T_c superconductors.

SUMMARY

We proposed a qualitative model of superconductivity, based on thermodynamics of a charged phase segregation. We described a superconductor as a segregated material with the quantized charge of tiny precipitates, which behave as charged bosonic quasiparticles. A Cooper pair was mentioned as an example of such quasiparticle. With cautions, our model can be viewed as a generalization of the conventional theory of superconductivity [3–7].

We pointed at instability of the electronic structure and the lattice as a cause for phase segregation. As an example, we considered instability at the Mott transition, around which we labeled 5 distinctive solid phases (shown in Figs. 3 and 4), two of which are superconductive.

We linked superconductivity with both the instability of the electronic structure and the lattice response to

variations of charge density. We claimed that a superconductor with a higher T_c has a larger lattice response, which can stabilize the charged bosonic quasiparticles at higher T . Thus, our model can be used in a guided search for novel high- T_c superconductors.

We acknowledge Paul C. Canfield and Duane D. Johnson for discussion. This work was supported in part by the U.S. Department of Energy (DOE), Office of Science, Basic Energy Sciences, Materials Science and Engineering Division. The research was performed at the Ames Laboratory, which is operated for the U.S. DOE by Iowa State University under contract # DE-AC02-07CH11358.

* zarkev@ameslab.gov

- [1] H. K. Onnes, in *Nobel Lectures* (1913).
- [2] A. A. Abrikosov, in *Nobel Lectures* (2003).
- [3] A. A. Abrikosov and L. P. Gor'kov, *Soviet Physics JETP* **35** (8), 1090 (1959), *ZhETF* 35, 1558–1571 (1958).
- [4] V. L. Ginzburg and L. D. Landau, *Zh. Eksp. Teor. Fiz.* **20**, 1064 (1950).
- [5] J. Bardeen, L. Cooper, and J. Schrieffer, *Phys. Rev.* **106**, 162 (1957), *Phys. Rev.* 108, 1175 (1957).
- [6] N. N. Bogoliubov, *Soviet Physics JETP* **34**, 41 (1958), *JETP* 34, 51 (1958); *ZhETF* 34, 58–65 and 73–79 (1958).
- [7] V. V. Tolmachev and S. V. Tiablikov, *Soviet Physics JETP* **34**, 46 (1958), *ZhETF* 34, 66–72 (1958).
- [8] L. P. Gor'kov, *Phys. Rev. B* **93**, 054517 (2016).
- [9] S. N. Bose, *Z. Phys.* **26**, 178 (1924).
- [10] N. F. Mott, *Proc. Phys. Soc. A* **62**, 416 (1949).
- [11] D. R. Lide, ed., *CRC Handbook of Chemistry and Physics*, 88th ed. (Taylor & Francis Group, Boca Raton, Florida, 2008).
- [12] P. C. Canfield, P. L. Gammel, and D. J. Bishop, *Physics Today* **51**, 40 (1998).
- [13] Y. Li, V. Baledent, G. Yu, N. Barisic, K. Hradil, R. A. Mole, Y. Sidis, P. Steffens, X. Zhao, P. Bourges, and M. Greven, *Nature* **468**, 283 (2010).
- [14] M. Zbiri, W. Jin, Y. Xiao, Y. Sun, Y. Su, S. Demirdis, and G. Cao, *Phys. Rev. B* **95**, 174301 (2017).
- [15] M. Zacharias, L. Bartosch, and M. Garst, *Phys. Rev. Lett.* **109**, 176401 (2012).
- [16] S. Medvedev, T. M. McQueen, I. A. Troyan, T. Palasyuk, M. I. Erements, R. J. Cava, S. Naghavi, F. Casper, V. Ksenofontov, G. Wortmann, and C. Felser, *Nat. Mater.* **8**, 630 (2009).
- [17] P. Phillips, *Phil. Trans. R. Soc. A* **369**, 1574 (2011).
- [18] M. Imada, A. Fujimori, and Y. Tokura, *Rev. Mod. Phys.* **70**, 1039 (1998).
- [19] M. S. Torikachvili, S. L. Bud'ko, N. Ni, and P. C. Canfield, *Phys. Rev. Lett.* **101**, 057006 (2008).
- [20] S. A. J. Kimber, A. Kreyssig, Y.-Z. Zhang, H. O. Jeschke, R. Valenti, F. Yokaichiya, E. Colombier, J. Yan, T. C. Hansen, T. Chatterji, R. J. McQueeney, P. C. Canfield, A. I. Goldman, and D. N. Argyriou, *Nat. Mater.* **8**, 471 (2009).
- [21] E. Lengyel, M. Kumar, W. Schnelle, A. Leithe-Jasper, and M. Nicklas, *Physica Status Solidi (b)* **254**, 1600154 (2017), 1600154.
- [22] S. Knöner, E. Gati, S. Köhler, B. Wolf, U. Tutsch, S. Ran, M. S. Torikachvili, S. L. Bud'ko, P. C. Canfield, and M. Lang, *Phys. Rev. B* **94**, 144513 (2016).
- [23] J.-H. Chu, J. G. Analytis, C. Kucharczyk, and I. R. Fisher, *Phys. Rev. B* **79**, 014506 (2009).
- [24] Z. Guguchia, R. Khasanov, Z. Bukowski, F. von Rohr, M. Medarde, P. K. Biswas, H. Luetkens, A. Amato, and E. Morenzoni, *Phys. Rev. B* **93**, 094513 (2016).
- [25] J.-H. Chu, J. G. Analytis, K. De Greve, P. L. McMahon, Z. Islam, Y. Yamamoto, and I. R. Fisher, *Science* **329**, 824 (2010).
- [26] J. Zhao, Q. Huang, C. de la Cruz, S. Li, J. W. Lynn, Y. Chen, M. A. Green, G. F. Chen, G. Li, Z. Li, J. L. Luo, N. L. Wang, and P. Dai, *Nat. Mater.* **7**, 953 (2008).
- [27] J. J. Wu, J. F. Lin, X. C. Wang, Q. Q. Liu, J. L. Zhu, Y. M. Xiao, P. Chow, and C. Q. Jin, *Scientific Reports* **4**, 3685 (2014).
- [28] V. Hlukhyy, A. V. Hoffmann, V. Grinenko, J. Scheiter, F. Hummel, D. Johrendt, and T. F. Fässler, *Physica Status Solidi (b)* **254**, 1600351 (2017).